Asian Journal of Chemistry; Vol. 26, No. 14 (2014), 4172-4176

ASIAN JOURNAL OF CHEMISTRY

http://dx.doi.org/10.14233/ajchem.2014.16054

Effect of TiC and TiC/Ti(C,N) Interlayer on Structure and Corrosion Properties of TiN Coating on 316L Stainless Steel Substrate

JIN ZHANG, QI XUE* and SONGXIA LI

School of Materials Science and Engineering, Southwest Petroleum University, Chengdu 610500, P.R. China

*Corresponding author: Fax: +86 28 83037406; Tel: +86 13320988644; E-mail: jzhang@swpu.edu.cn

Received: 16 July 2013; *Accepted*: 29 October 2013; *Published online*: 5 July 2014; AJC-15435

This paper focuses on the research of preparing TiN, TiC/TiN, TiC/Ti($C_{0.3}$,$N_{0.7}$)/TiN films on 316L stainless steel substrates by the method of high temperature chemical vapor deposition. The phase structure, surface and cross section morphology of the deposited films have been analyzed and illustrated. Compared with TiN and TiC/TiN coating, the TiC/ Ti($C_{0.3}$,$N_{0.7}$)/TiN coating exhibits enhanced adhesion between TiN coating and the substrates. Based on the corrosion measurement, it can be concluded that the coating samples exhibit better corrosion resistance in 20 % H_2SO_4 solution at room temperature. The TiC/ Ti($C_{0.3}$,$N_{0.7}$)/TiN coating specially exhibits the best adhesion and corrosion resistance which is beneficial for the future application of 316L stainless steel.

Keywords: HTCVD, Corrosion resistance, Multilayer coatings, 316L stainless steel, Adhesion.

INTRODUCTION

Due to its superior corrosion resistance, high toughness and biocompatibility, 316L stainless steel has been used extensively in many fields such as oil extraction, chemical industry, atomic energy application and biomedical implants[1,2]. Up to now, improving the corrosion resistance and biocompatibility of the 316L stainless steel for it being used in a wide range of atmospheric environments and corrosive media is still a challengeable, important and necessary research field. Thus, a variety of surface treatments such as surface coating, electrochemical polishing (EP)[3] and plasma nitro carburizing[4] have been performed on 316L stainless steel. Among the coating materials, titanium nitride exhibits a good corrosion resistance and has been widely used in cutting tools and wear parts[5,6]. Ti(C, N) coating (a series of TiC_xN_{1-x} films, $0 < x < 1$) even exhibits a better abrasive wear resistance[7]. Currently, the extension of these hard transition metal compounds towards more versatile multi-layers or gradient layers with even better performance is widely investigated[8,9]. A variety of methods including magnetron sputtering[10,11], vacuum arc deposition and nitrogen ion beam dynamic mixing implantation[12,13], ion-plating[14], PIII & D as well as chemical vapour deposition have been used to deposit these films on different substrate materials[15,16,17]. There are also reports on surface modification of 316L stainless steel which is coated with those ceramic materials to improve the anti-corrosion property of the surface[18,19]. High temperature chemical vapour deposition (HTCVD) is a novel and simple method that can not only enhance bonding strength between the coatings and substrates, but also easily control the deposition rate of the film[20]. However, there are hardly any reports to comparison with structural, morphological and corrosion characteristics between TiN monolayer and Ti (C, N) multilayer coatings on 316L stainless steel by high temperature chemical vapor deposition method. These studies would be useful for understanding the advantages of growing films as bilayer or multilayer rather than monolayer.

In this work, TiN, TiC/TiN and TiC/Ti($C_{0.3}$,$N_{0.7}$)/TiN films were deposited on 316L stainless steel by high temperature chemical vapor deposition method. The structure, morphology and adhesion of the coatings were analyzed and illustrated. In addition, the corrosion behaviour of the different coatings was evaluated in 20 % H_2SO_4 solution through potentiodynamic polarization technique.

EXPERIMENTAL

Substrates were made out of 316L stainless steel (16.9 % Cr, 14.5 % Ni, 2.2 % Mo, 1.14 % Mn, 0.2 % Si, 0.02 % C, Fe balanced all, in wt. %) and machined to Φ 20 mm × 3 mm in size. Prior to the coating process, the specimens were polished with emery paper of 600 grit, cleaned in ultrasonic bath with acetone, sodium hydroxide solution and deionized water. During the coating treatments, working gas generally consists of carrier gas hydrogen (H_2) and reactive gases depending on the layers to be deposited. In the case of TiN, nitrogen (N_2) is used; for TiC, methane (CH_4) is added; a mixture of the two is

TABLE-1
PROCESSING PARAMETERS OF THE FILMS

	Gas flow (%)	Thickness and deposition time	Constant parameters
Coating	N_2: 35 mol H_2: 56 mol $TiCl_4$: 9 mol	TiN layer: 4 μm; 1.5 h	Deposition temperature: 1050 °C
TiC	CH_4: 10 mol H_2: 85 mol $TiCl_4$: 5 mol	TiC/TiN:1 μm/3 μm; 40 min/1 h	Deposition pressure: 0.01 MPa
$Ti(C_{0.3}N_{0.7})$	N_2: 30 mol CH_4: 7 mol H_2: 55 mol $TiCl_4$: 8 mol	TiC/$Ti(C_{0.3}N_{0.7})$/TiN: 1 μm/2 μm/3 μm; 40 min/30 min/50 min	System cooling: 10 °C/min in H_2 atmosphere Sandblast pressure: 0.4 MPa

employed for Ti(C, N) layer deposition. Titanium tetrachloride is used as metal donor substance during the process. The main process parameters are given in Table-1.

CuK_α radiation (λ = 1.54178 Å) in the θ-2θ scan mode (DX1000, Dandong, China) is used for the X-ray diffraction (XRD) characterization of the multilayer films. The cross-section and surface morphology of the films were observed by a scanning electron microscope (SEM, JSM-5900, Japan). Film/substrate adhesion was investigated by scratching testing instrument(MFT-4000, Lanzhou, China). A diamond tip was used to scratch the film surface with a loading speed 100 N/min, horizontal velocity 4 mm/min, the maximum scratching length 10 mm.The acoustic signal (AE-acoustic emission) was recorded as the adhesion evaluation when the film was broken by the tip. The electrochemical measurements were performed in a standard three-electrode cell, with a 1 cm^2 platinum counter electrode and a saturated calomel electrode (SCE) as the reference. The electrolyte is 20 % H_2SO_4 solution. All the corrosion experiments were carried out *via* the Auto-lab PG302 Potentiostat Electrochemistry Workstation at room temperature.

RESULTS AND DISCUSSION

Phase structure and morphology of the films: Figs. 1-3 show the XRD patterns of the as-deposited TiN, TiC/TiN, TiC/$Ti(C_{0.3},N_{0.7})$/TiN films, respectively. For the deposited TiN single layer, the XRD pattern shown in Fig.1 reveals that diffraction peaks of TiN phase can also be found apart from the diffraction peaks of 316L stainless steel. As for the deposited TiC/TiN bilayer films, Fig. 2 indicates that only TiC phase and TiN phase can be indexed in the corresponding X-ray diffraction spectrum. The diffraction peaks of TiN phase and TiC phase are consistent with the standard JCPDS data. The XRD measurements indicate the high phase purity of our deposited TiN and TiC/TiN films. However, for the deposited TiC/$Ti(C_{0.3},N_{0.7})$/TiN multi-layer films, Fig. 3 shows that the residual peaks can be indexed to a newly formed $Cr_{23}C_6$ phase besides the diffraction peaks corresponding to the required TiC, TiN and $Ti(C_{0.3}N_{0.7})$ phase. It indicates that during the high temperature depositing process, carbon element firstly diffuses through TiC layer and furthermore diffuses into 316L stainless steel substrate and then it combines with the Cr element to form the $Cr_{23}C_6$ phase. As reported by Sebire *et al.*[21], the significant chemical inter-diffusion between the coating and the substrate could be optimize boundary structure and improve the critical load.

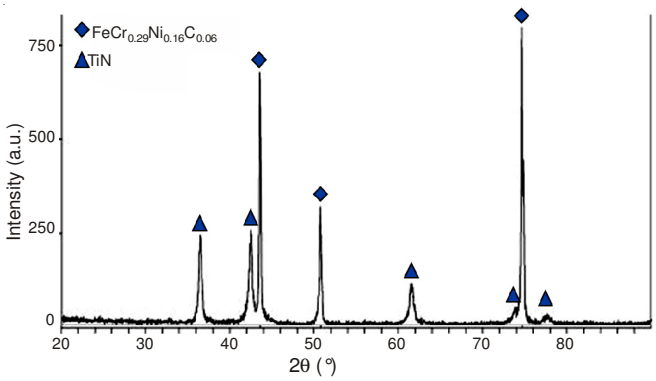

Fig. 1. XRD pattern of the as-deposited TiN film on 316L stainless steel substrate

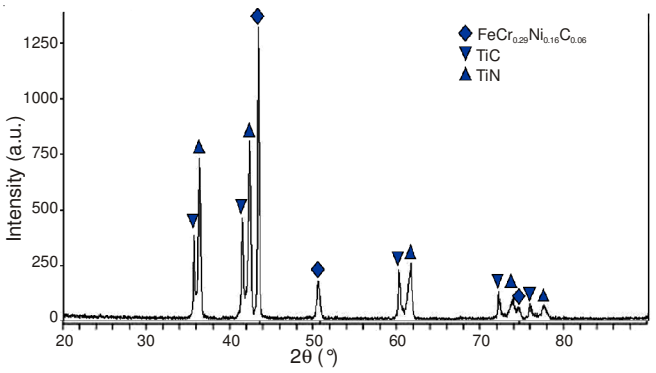

Fig. 2. XRD pattern of the as-deposited TiC/TiN bilayer films on 316L stainless steel substrate

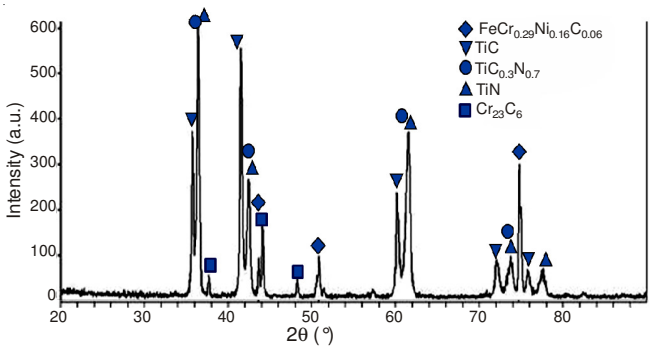

Fig. 3. XRD pattern of the as-deposited TiC/$Ti(C_{0.3}N_{0.7})$/TiN multi-layer films on 316L stainless steel substrate

The morphology of the TiN, TiC/TiN and TiC/Ti($C_{0.3}N_{0.7}$)/TiN films deposited on 316L stainless steel are shown in Figs. 4-6, respectively. The cross-section and surface morphology of the TiN layers are shown in Fig. 4a and b respectively. It can be clearly observed that cracks with width about 0.4 μm divided the deposited TiN film into many square or erose pieces. The cracks might be formed because of the large difference of thermal expansion coefficient between the TiN layer and the steel substrate. The larger is the expansion coefficient difference between the film and the substrate, the bigger the thermal stress of the film system[22]. For the TiC/TiN film as shown in Fig. 5, cracks also can be found, but they are much thinner and with much smaller density. The surface of the TiC/TiN films has a structure of roughness and hollowness. The addition of the TiC layer made the TiC/TiN layer more compact which might exhibit better adhesion and anti-corrosion properties. Fig. 6 shows the surface morphology of the TiC/Ti($C_{0.3}N_{0.7}$)/TiN layer. Numerous needle-like structures can be found at the surface of the film. These "needles" with lengths of about 1μm lay randomly across each other, which may enhance the adhesion between the layers and the substrate.

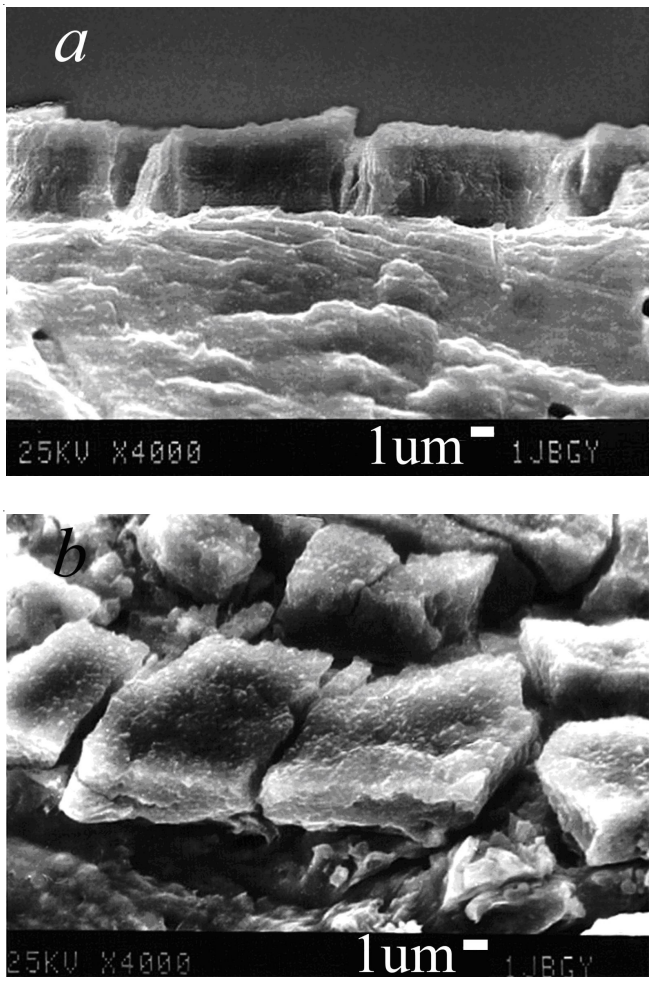

Fig. 4. SEM images of the as-deposited TiC film on 316L stainless steel substrate (a) Cross-section morphology. (b) Surface morphology

Adhesion of the films: The scratch testing has been applied to determine the adhesion of the coatings deposited on the steel substrates[23]. Figs. 7 and 8 present the curves of acoustic emission (AE) corresponding to TiC/TiN layer and TiC/Ti($C_{0.3}N_{0.7}$)/TiN layer. Fig. 7 presents that the layer began to break when the force of 25N is applied. In the case of the TiC/Ti($C_{0.3}N_{0.7}$)/TiN system, the changes in the curves of AE (Fig. 8) indicate that the peeling off of the multi-layers occurs at about 50N, which is without the stage of bond destruction in the interface $TiC_{0.3}N_{0.7}$-TiN and $TiC_{0.3}N_{0.7}$-TiC. It indicates that all the three layers are peeled off from steel substrate simultaneously. The increasing adhesion values of TiC/Ti($C_{0.3}N_{0.7}$)/TiN multilayer films could be seen to correlate in a significant manner with the multilayer structure[24,25]. In this mechanism multilayer interface serves as crack tip deflectors which change the direction of the initial crack when it penetrates deep into the coating and strengthens the multilayer coatings systems.

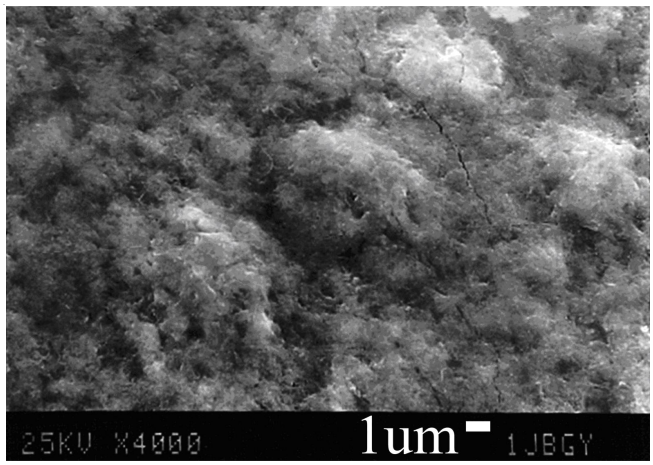

Fig. 5. SEM image of the TiC/TiN bilayer films on 316L stainless steel substrate

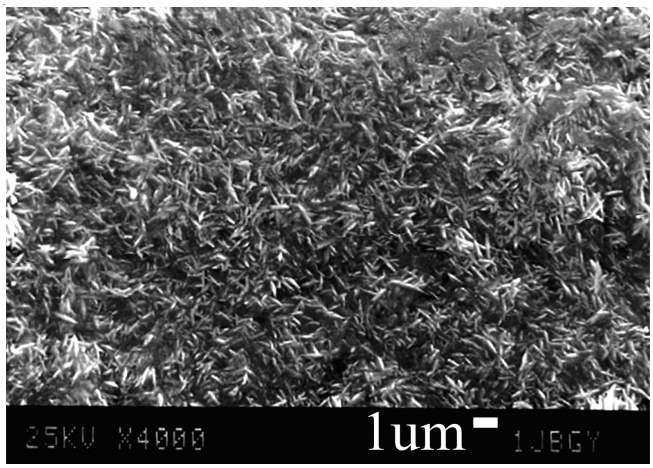

Fig. 6. SEM image of the TiC/Ti($C_{0.3}N_{0.7}$)/TiN multi-layer films on the 316L stainless steel substrate

Corrosion behavior of the films: The anodic polarization curves for the coated and uncoated samples are shown in Fig. 9. TiC film was also deposited for the comparison the corrosion properties. Table-2 shows the corrosion potential, corrosion current density and polarization resistance of the five different types of the films which were calculated according to the polarization curves. As shown in Table-2, the coated films deposited by this HTCVD method exhibit relatively high corrosion resistance, low corrosion potential and low corrosion current density. The corrosion potential and corrosion resistance ranged

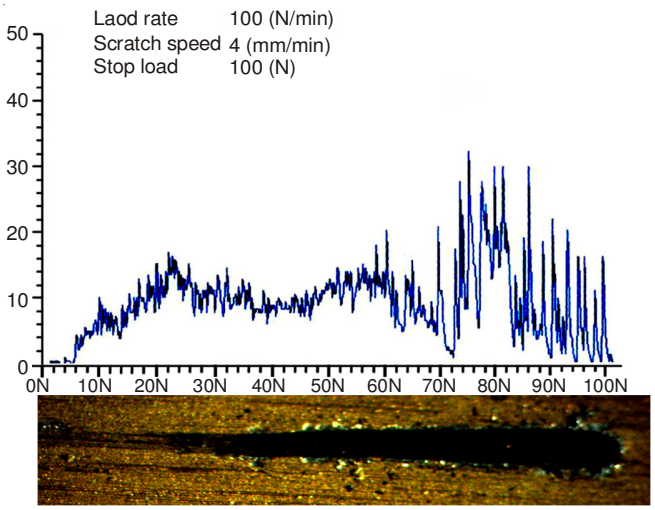

Fig. 7. Acoustic emission curve for TiC/TiN films deposited on 316L stainless steel

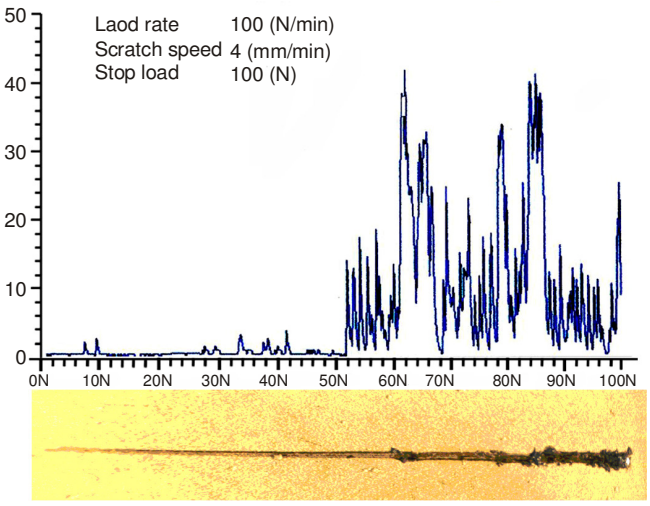

Fig. 8. Acoustic emission curve for TiC/Ti($C_{0.3}N_{0.7}$)/TiN films deposited on 316L stainless steel

from low to high values in the order of steel, TiC, TiN, TiC/TiN and TiC/Ti($C_{0.3}N_{0.7}$)/TiN. The corrosion potential/polarization resistance for the uncoated specimen is about -0.422V/623O cm^{-2} and -0.286V/1687O cm^{-2} for the TiC/Ti($C_{0.3}N_{0.7}$)/TiN coated specimen. This fact indicates that the uncoated sample has the lowest thermal dynamic stability, whereas the sample coated with TiC/Ti($C_{0.3}N_{0.7}$)/TiN is more stable compared to that of other specimens.

As clearly shown in Fig. 9, the uncoated sample (curve E) has the highest passive current density of about 4×10^{-4} to 8×10^{-1} A/cm^2 in the range from -0.450 mV to 0.200 mV. For the samples coated with TiC/TiN (curve B) and TiC/Ti($C_{0.3}N_{0.7}$)/TiN (curve A) films, their anodic polarization curves are almost similar with a wide passive range. But it is worth noting that the passive current density of TiC/TiN coated sample is higher than that of the TiC/Ti($C_{0.3}N_{0.7}$)/TiN coated sample. For the steel coated with TiN (curve C) and TiC (curve D) film only, the anodic polarization behavior can be divided into two stages. At the initial stage, the current density rapidly increases with the potential increase from -360 mV to 200 mV. After the potential reaches 200 mV, the current density increases from 2×10^{-2} A/cm^2 to 5×10^{-1} A/cm^2 and then increases slowly with the increase of applied potential, exhibiting the passive state. By analyzing the results of the anodic polarization experiments, we found that the corrosion resistance of the coated samples is improved and the TiC/Ti($C_{0.3}N_{0.7}$)/TiN coated sample is the best among them.

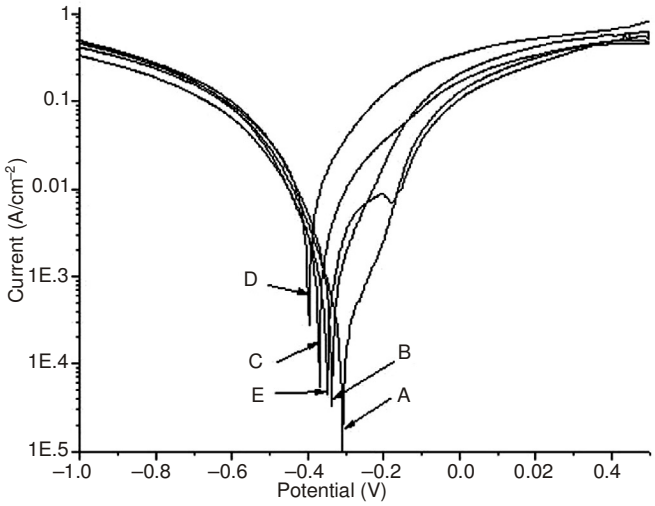

Fig. 9. Polarization curve of the different films: TiC/Ti($C_{0.3}N_{0.7}$)/TiN (A), TiC/TiN (B), TiN (C), TiC(D), bare 316L stainless steel (E)

Conclusion

In summary, TiN, TiC/TiN and TiC/ Ti($C_{0.3}$, $N_{0.7}$)/TiN films have been deposited on 316L stainless steel by the HTCVD method. The structure, morphology, adhesion and corrosion resistance of the coatings have been illustrated and analysed. It can be concluded that the coating samples exhibit better adhesive behavior and corrosion resistance. Especially the TiC/Ti($C_{0.3}$,$N_{0.7}$)/TiN coating exhibits the best adhesion and corrosion resistance which is beneficial for the future application of 316L stainless steel.

ACKNOWLEDGEMENTS

The authors thank The National High Technology Research and Development Program of China (863 program) (No. 2007AA-09Z202) and Foundation of Sichuan Educational Committee (No.2012ZB164) for financial supports to the work.

TABLE-2
CORROSION POTENTIAL, CORROSION CURRENT DENSITY, AND POLARIZATION RESISTANCE OF THE TiN, TiC/TiN, TiC/Ti($C_{0.3}N_{0.7}$)/TiN FILMS AND THE STEEL SUBSTRATE

	TiC/Ti($C_{0.3}N_{0.7}$)/TiN (A)	TiC/TiN (B)	TiN (C)	TiC (D)	316L steel (E)
Corrosion potential (V)	-0.286	-0.326	-0.359	-0.383	-0.422
Polarization resistance (Ω cm^{-2})	1687	1351	1058	913.3	623
Corrosion current density (mA cm^{-2})	7.109	12.87	21.68	31.8	38.67

REFERENCES

1. T. Hryniewicz, R. Rokicki and K. Rokosz, *Surf. Coat. Techol*., **202**, 1668 (2008).
2. L. Chenglong, Y. Dazhi, L. Guoqiang and Q. Min, *Mater. Lett*., **59**, 3813 (2005).
3. T. Hryniewicz, K. Rokosz and R. Rokicki, *Corros. Sci*., **50**, 2676 (2008).
4. C.N. Chang and F.S. Chen, *Mater. Chem. Phys*., **82**, 281 (2003).
5. E.I. Meletis, C.A. Gibbs and K. Lian, *Dent. Mater*., **5**, 411 (1989).
6. P.K. Ajikumar, M. Kamruddin, S. Kalavathi, A.K. Balamurugan, S. Kataria, P. Shankar and A.K. Tyagi, *Ceram. Int*., **38**, 2253 (2012).
7. M. Yasuoka, P.P. Wang and R.I. Murakami, *Surf. Coat. Technol*., **206**, 2168 (2012).
8. L. Ipaz, J.C. Caicedo, J. Esteve, F.J. Espinoza-Beltran and G. Zambrano, *Appl. Surf. Sci*., **258**, 3805 (2012).
9. J. Smolik and K. Zdunek, *Surf. Coat. Technol*., **116-119**, 398 (1999).
10. L.F. Senna, C.A. Achete, T. Hirsch and F.L. Freire Jr., *Surf. Coat. Technol*., **94-95**, 390 (1997).
11. J.C. Caicedo, C. Amaya, G. Cabrera, J. Esteve, W. Aperador, M.E. Gomez and P. Prieto, *Thin Solid Films*, **519**, 6362 (2011).
12. C.S. Ren, Z.X. Mu, Y.N. Wang and H. Yu, *Surf. Coat. Technol*., **185**, 210 (2004).
13. D.M. Devia, E. Restrepo-Parra and P.J. Arango, *Appl. Surf. Sci*., **258**, 1164 (2011).
14. J.Y. Chen, G.P. Yu and J.H. Huang, *Mater. Chem. Phys*., **65**, 310 (2000).
15. S.K. Kim, T.H. Kim, J. Wöhle and K.-T. Rie, *Surf. Coat. Technol*., **131**, 121 (2000).
16. T. Miller, J.-M. Lin, L. Pirolli, L. Coquilleau, R. Luharuka and A.V. Teplyakov, *Thin Solid Films*, **522**, 193 (2012).
17. J. Garcia, R. Pitonak, L. Agudo and A. Kostka, *Mater. Lett*., **68**, 71 (2012).
18. L. Chenglong, Y. Dazhi, L. Guoqiang and Q. Min, *Mater. Lett*., **59**, 3813 (2005).
19. M.C. Li, S.Z. Luo, C.L. Zeng, J. Shen, H. Lin and C. Cao, *Corros. Sci*., **46**, 1369 (2004).
20. R. Yigit, E. Celik, F. Findik and S. Koksal, *Int. J. Refract. Met. Hard Mater*., **26**, 514 (2008).
21. I. Lhermitte-Sebire, R. Colmet, R. Naslain, J. Desmaison and G. Gladel, *Thin Solid Film*, **138**, 221 (1986).
22. Y.H. Zhao, G.Q. Lin, J.Q. Xiao, C. Dong and L.S. Wen, *Vacuum*, **85**, 1 (2010).
23. H. Jensen, U.M. Jensen and G. Sorensen, *Surf. Coat. Technol*., **74-75**, 297 (1995).
24. C. Subramanian and K.N. Strafford, *Wear*, **165**, 85 (1993).
25. L. Ipaz, J.C. Caicedo, J. Esteve, F.J. Espinoza-Beltran and G. Zambrano, *Appl. Surf. Sci*., **258**, 3805 (2012).